design concepts, Purdue University, School of Mechanical Engineering, Technical Report No. ME-HTL-75-2 (December 1975).
12. R. Viskanta and E. D. Hirleman, Solar radiation transmission and heat transfer through architectural windows, in *Heat and Mass Transfer in Buildings*, Edited by J. C. Hoogedorn. Hemisphere, Washington, D.C. (in press).
13. R. Siegel and J. R. Howell, *Thermal Radiation Heat Transfer*. McGraw-Hill, New York (1972).
14. PPG Industries, Float glass, Glass Division/PPG Technical Services, PDS-fl, Pittsburgh, PA (1972).
15. Libbey–Owens–Ford Co., Glass for construction, Report LOF8.2/Li, Toledo, Ohio (1977).
16. *Handbook of Geophysics*, Revised ed. pp. 16 19. McMillan, New York (1960).
17. H. Schröder, "Grossflächenbelegung von Glas zur Änderung der Strahlungsdurchläsigkeit," *Glastech. Ber.* **39**, 156–165 (1966).
18. S. M. Berman and S. D. Silverstein (editors), *Energy Conversion and Window Systems*. American Physical Society, New York (1975).

Int. J. Heat Mass Transfer. Vol. 21, pp. 818–821

0017-9310/78/0601-0818 $02.00/0

ANALYTIC INCORPORATION OF PROBABILITY DENSITY FUNCTIONS IN TURBULENT FLAMES*

T. M. SHIH and P. J. PAGNI
Department of Mechanical Engineering, University of California, Berkeley, CA 94720, U.S.A.

(*Received* 25 *April* 1977 *and in revised form* 14 *November* 1977)

NOMENCLATURE

- C_p, specific heat;
- D_3, third Damköhler number, $Q_p Y_{ox,\infty}/h_0$;
- J, time-mean normalized Shvab–Zeldovich concentration, $(\beta-\beta_\infty)/(\beta_0-\beta_\infty)$ or $(\gamma-\gamma_\infty)/(\gamma_0-\gamma_\infty)$;
- $\tilde{J}$, instantaneous J;
- J', fluctuation of J, $\tilde{J}-J$;
- g, $\overline{(J')^2}$;
- h, enthalpy;
- M, molecular weight;
- $P(\tilde{J})$, probability density function;
- Q_p, heat of reaction per g of oxygen;
- r, mass consumption number, $Y_{ox,\infty}\nu_f M_f/Y_{f,0}\nu_{ox}M_{ox}$;
- T, temperature;
- Y, mass fraction;
- z, $(\tilde{J}-\mu)/\sigma(2)^{1/2}$.

Greek symbols

- β, γ, S–Z variable, $Y_f/\nu_f M_f - Y_{ox}/\nu_{ox}M_{ox}$ or $-h/Q_p\nu_{ox}M_{ox} - Y_{ox}/\nu_{ox}M_{ox}$;
- μ, viscosity, or most probable value of $\tilde{J}$;
- ν, stoichiometric coefficient;
- ρ, density;
- σ, standard deviation of Gaussian distribution.

Subscripts

- 0, reference, i.e. wall, initial, etc.;
- ox, oxygen;
- 0.5, locations where $Y_{ox}/Y_{ox,\infty} = 0.5$;
- ∞, ambient.

SEVERAL investigators have assumed a probability density function (pdf) for the instantaneous Shvab–Zeldovich concentration variable $\tilde{J}$ in a turbulent diffusion flame. The problem is to recover the oxygen concentration Y_{ox}, fuel concentration Y_f, enthalpy h, and density ρ from the pdf for $\tilde{J}$. Spalding [1] initiated the concentration fluctuation model and Elghobashi and Pun [2], Lockwood and Naguib [3], Shih and Pagni [4] and Tamanini [5] have applied Spalding's model to flame phenomena. A clipped Gaussian curve, characterized by a most probable value μ and a standard deviation σ, as shown in Fig. 1, is assumed. The values of J and g, obtained numerically at each grid node in the flow field, implicitly specify μ and σ which then define $\tilde{Y}_{ox}$, $\tilde{Y}_f$, $\tilde{h}$ and $\tilde{\rho}$ and their time-means for flows where $\tilde{\beta}$ and $\tilde{\gamma}$ obey the same equations and conditions. However, the implicit nature of these expressions requires inconvenient and expensive numerical calculations. This motivated the present study which utilizes the character of the Gaussian pdf to provide direct explicit expressions for Y_{ox}, Y_f, h, and ρ in terms of J mainly and g weakly. The two parameters, μ and σ, which play minor roles in the physical system are eliminated from the numerical procedure.

It has been observed [6–8] that the instantaneous fluctuations due to turbulence can often be represented with a Gaussian distribution. The clipped form for the instantaneous Shvab–Zeldovich concentration is written as

$$P(\tilde{J}) = \frac{R(z)}{\sigma(2\pi)^{1/2}}[U(\tilde{J})-U(\tilde{J}-1)] + \tfrac{1}{2}\{[1+\mathrm{erf}(z_1)]\delta(\tilde{J}) + \mathrm{erfc}(z_0)\delta(1-\tilde{J})\} \quad (1)$$

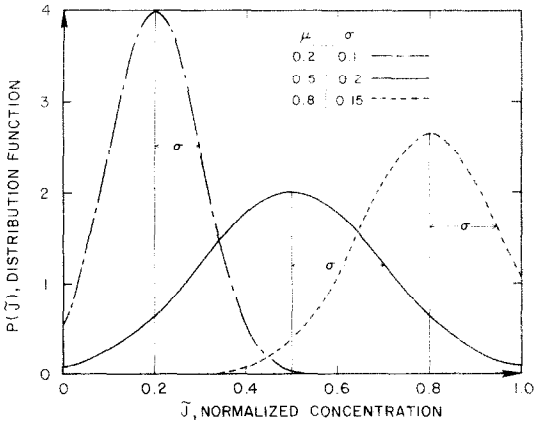

FIG. 1. Typical clipped Gaussian probability density functions are shown for a wide range of physical conditions.

*The authors are grateful for support from the National Bureau of Standards, Fire Research Center and the Products Research Committee. Many valuable comments by Dr. F. Tamanini are much appreciated. The opinions expressed herein are those of the authors and not of the Products Research Committee.

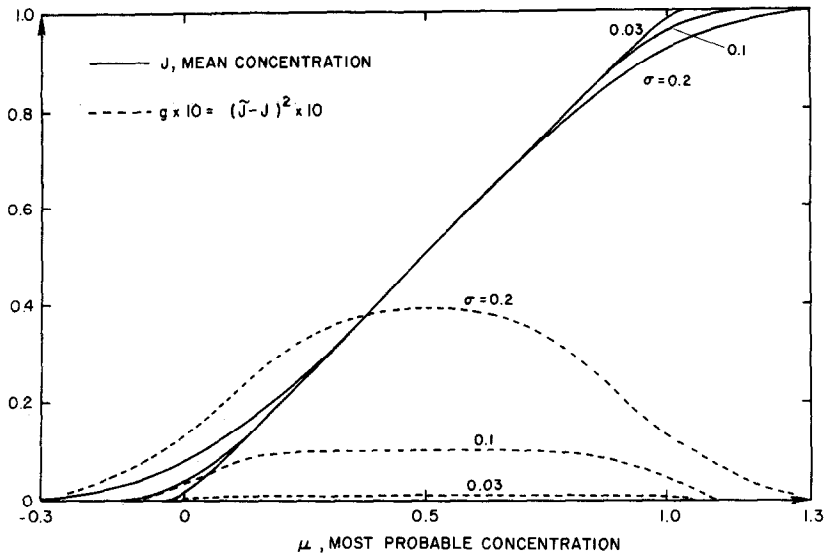

FIG. 2. Time-mean Shvab–Zeldovich concentration and squared concentration fluctuation are shown as functions of the most probable $\tilde{J}$ parameterized in the standard deviation of $\tilde{J}$.

where

$$R(z) = \exp(-z^2),\ z_\infty = -\frac{\mu}{\sigma(2)^{1/2}} \text{ and } z_0 = \frac{1-\mu}{\sigma(2)^{1/2}}.$$

$U(t)$ is the unit-step function used to restrict $\tilde{J}$ to $0 \leqslant \tilde{J} \leqslant 1$, and $\delta(t)$ is the Dirac delta function used to normalize the distribution.

Figure 1 shows three typical distributions which, from left to right, correspond physically to the probabilities of $\tilde{J}$ for flows near ambient conditions, a reaction region, and fuel-rich region. The fluctuations and thus the standard deviation σ are largest within the flame brush where the largest mean concentration gradient and therefore the maximum production of fluctuations occurs.

Any time-mean quantity ϕ can be evaluated using

$$\phi = \int_0^1 \tilde{\phi}(\tilde{J})P(\tilde{J})\,\mathrm{d}\tilde{J}. \tag{2}$$

From equation (2) and integration by parts, one obtains

$$J(\mu,\sigma) = \tfrac{1}{2}[1-\mu\,\mathrm{erf}(z_\infty)-(1-\mu)\mathrm{erf}(z_0)] + \frac{\sigma}{(2\pi)^{1/2}}[R(z_\infty)-R(z_0)], \tag{3}$$

and

$$g(\mu,\sigma) = \tfrac{1}{2}\{1-\mathrm{erf}(z_0)-(\mu^2+\sigma^2)[\mathrm{erf}(z_\infty)-\mathrm{erf}(z_0)]\} + \frac{\sigma}{(\pi)^{1/2}}\{[z_\infty\sigma+(2)^{1/2}\mu]R(z_\infty) - [z_0\sigma+(2)^{1/2}\mu]R(z_0)\} - J^2. \tag{4}$$

Equations (3) and (4) are plotted in Fig. 2. In the range $0.3 \lesssim \mu \lesssim 0.7$, the time-mean value, J, is equal to the most probable value μ. For extreme values of μ or large σ, since more area under the Gaussian curve is clipped, J deviates more from μ. In the laminar case where $\sigma = 0$, J equals μ always. The extremes $\mu \leqslant 0$ and $\mu \geqslant 1$ occur in unmixed regions. In principle, equations (3) and (4) or Fig. 2 can yield a table of μ and σ in terms of the variables J and g which are numerically obtained at each grid node from the turbulent flame analysis [2, 3, 5]. The interpolated values of μ and σ from the table subsequently yield Y_{ox}, Y_f, h and ρ through equation (2). This calculation procedure is inevitably complex.

The present study seeks explicit expressions for Y_{ox}, Y_f, h and ρ in terms of J and g. It is easily shown that if a quantity $\tilde{\phi}$ varies Gaussianally in the interval $a \leqslant \tilde{\phi} \leqslant b$, the most probable $\tilde{\phi}$ coincides with the mean $\tilde{\phi}$ when the mean $\tilde{\phi}$ equals $0.5(a+b)$. The solid curve in Fig. 1, for $\mu = 0.5$, shows that, since the distribution is assumed Gaussian, $J = \mu = 0.5$ regardless of the variation of σ. This behavior, due to symmetric tail clipping when $\mu = 0.5$, is very useful.

Assuming infinite kinetics, equations (2) and (3) with the definitions of $\tilde{J}$ and β give the time-mean oxygen concentration as

$$Y_{ox}(\mu,\sigma,r)/Y_{ox,\infty} = \tfrac{1}{2}\{1+\mathrm{erf}(z_s)+(\mu+\mu/r)[\mathrm{erf}(z_0)-\mathrm{erf}(z_s)]\} + (\sigma+\sigma/r)[R(z_s)-R(z_0)]/(2\pi)^{1/2} \tag{5}$$

where

$$z_s = \left(\frac{r}{1+r}-\mu\right)\Big/\sigma(2)^{1/2}$$

and

$$r = Y_{ox,\infty}\nu_f M_f / Y_{f,0}\nu_{ox}M_{ox}.$$

The mass consumption number, r, defined as the ratio of the relative available oxygen $Y_{ox,\infty}/Y_{f,0}$ to the stoichiometrically required oxygen $\nu_{ox}M_{ox}/\nu_f M_f$ [9] plays an important role in both laminar and turbulent diffusion flame analyses. Whenever Y_{ox}, Y_f and h are recovered from the Shvab–Zeldovich concentration J, this parameter r will appear in expressions such as equation (5). Again from the definition of $\tilde{J}$ and equation (2), the other time-mean variables are obtained in terms of J and Y_{ox} as:

$$Y_f/Y_{f,0} = (1+r)J - r(1-Y_{ox}/Y_{ox,\infty}), \tag{6}$$

$$h/h_0 = (1-D_3)J + D_3(1-Y_{ox}/Y_{ox,\infty}), \tag{7}$$

and

$$\rho/\rho_0 = (1+C_pT_\infty/h_0)/(h/h_0+C_pT_\infty/h_0) \tag{8}$$

where

$$h = \int_{T_\infty}^{T} C_p\,\mathrm{d}T \simeq C_p(T-T_\infty) \text{ and } T'/T \ll 1$$

are assumed in equation (8). Since $\tilde{Y}_{ox}$ varies from zero to $Y_{ox,\infty}$, Y_{ox} coincides with the most probable $\tilde{Y}_{ox}$ when $Y_{ox} = 0.5Y_{ox,\infty}$ for all values of σ. The value of μ corresponding to $Y_{ox} = 0.5Y_{ox,\infty}$ is obtained from equation (5) as

$$\mu_{0.5} = r/2(1+r). \tag{9}$$

This variable helps exploit the symmetry of the assumed distribution. Once $Y_{ox,\infty}$ and the fuel are specified, $\mu_{0.5}$ is specified; typically, $0 \lesssim \mu_{0.5} \lesssim 0.3$.

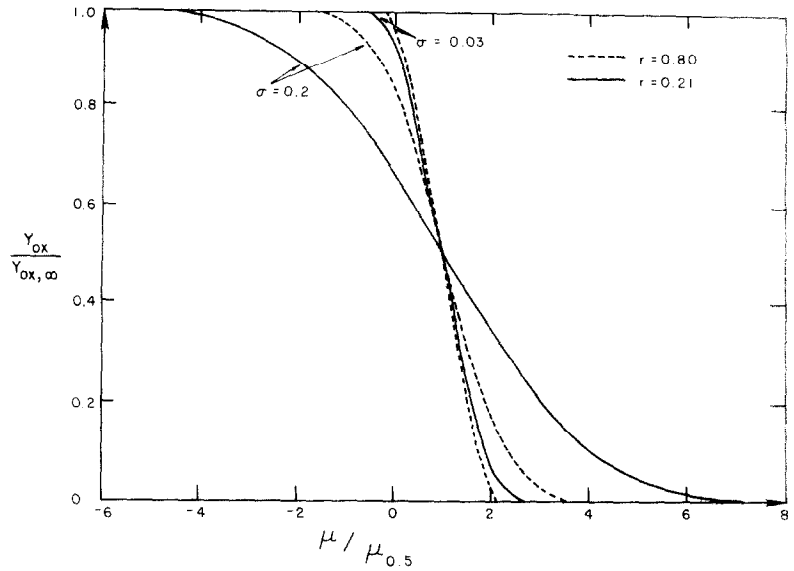

FIG. 3. Normalized oxygen concentration is shown as a function of normalized μ parameterized in the standard deviation of J.

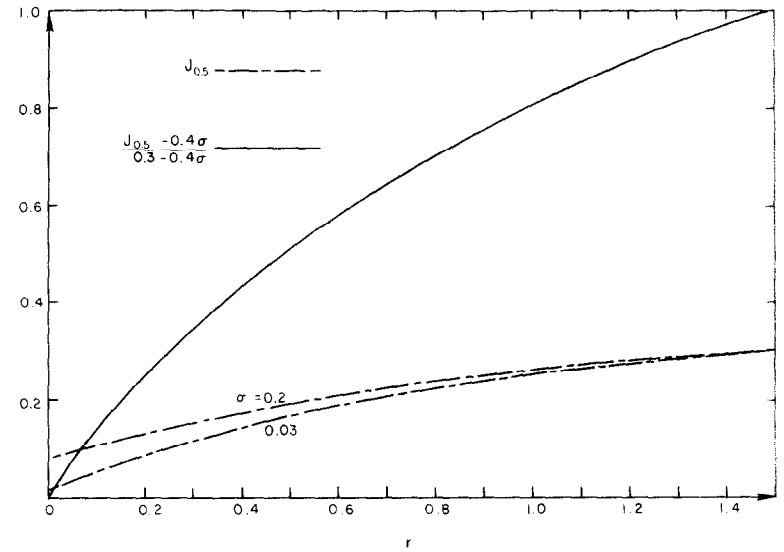

FIG. 4. $J_{0.5}$ is shown as a function of the mass consumption number parameterized in the standard deviation. The weak σ dependence is eliminated when $J_{0.5}$ is suitably normalized.

Since equations (6)–(8) are only functions of Y_{ox} and J, a simple expression for $Y_{ox}(J, g)$ would provide all the desired species and temperature variables explicitly in terms of J and g. Finding this $Y_{ox}(J, g)$ is accomplished by converting the independent variables μ and σ in equation (5) to J and g. Figure 3 shows $Y_{ox}/Y_{ox,\infty}$ as a function of $\mu/\mu_{0.5}$ parameterized in σ. The similarity among these curves, which converge at $Y_{ox}/Y_{ox,\infty} = 0.5$ and $\mu/\mu_{0.5} = 1$, suggests representing all distributions with a single curve. Consider first the region $\mu \leqslant \mu_{0.5}$. Odd symmetry will later be used to obtain the region $\mu > \mu_{0.5}$.

J is a more natural variable than μ to describe $Y_{ox}/Y_{ox,\infty}$ since both Y_{ox} and J are time-mean values. In this form the σ-dependence becomes weak and μ is eliminated from the analysis. The distributions shown in Fig. 3 are approximated by a single equation when J is normalized on $J_{0.5}$, the value of J when $Y_{ox}/Y_{ox,\infty} = 0.5$. This expression is

$$Y_{ox}/Y_{ox,\infty} = 1 - J/2J_{0.5}, \text{ for } 0 \leqslant J \leqslant J_{0.5} \quad (10)$$

where

$$J_{0.5} \approx (2.67\mu_{0.5} + 2.22\mu_{0.5}^2)(0.3 - 0.4\sigma) + 0.4\sigma \quad (11)$$

and

$$\sigma \approx g^{1/2}(0.34 + 4.55\mu_{0.5} - 10.29\mu_{0.5}^2 + 7.65\mu_{0.5}^3)^{-1/2} \quad (12)$$

are obtained by curve-fitting.

Figure 4 shows $J_{0.5}$ from equations (3) and (9) parameterized in σ. It was noted that $J(0, \sigma) \approx 0.4\sigma$ and $J(0.3, \sigma) \approx 0.3$ and that $[J_{0.5} - J(0, \sigma)]/[J(0.3, \sigma) - J(0, \sigma)]$ is approximated by the first polynomial on the right of equation (11), also shown in Fig. 4. Since $J_{0.5}$ is nearly linear in $\mu_{0.5}$, second order suffices. The four coefficients in equation (12) were chosen to satisfy four arbitrary conditions on $g(\mu, \sigma)$ from equation (4): $g(0, \sigma) = 0.34\sigma^2$, $g(0.1, \sigma) = 0.75\sigma^2$, $g(0.2, \sigma) = 0.97\sigma^2$ and $g(0.5, \sigma) = \sigma^2$. Third order adequately represents $\sigma(\mu_{0.5})$. Equations (11) and (12) appear accurate to within 2% for all μ and $\sigma < 0.2$. The error in Y_{ox} is $J/2J_{0.5}^2$ times the error in $J_{0.5}$. Equations (10)–(12), called here the "flame-brush profile equations" are key results in this analysis. They can be used to evaluate Y_{ox} and thus Y_f, h and ρ directly from J and g without obtaining the intermediates μ and σ.

Now consider the region $\mu_{0.5} < \mu$, i.e. $J_{0.5} < J \leqslant J(2\mu_{0.5}, \sigma)$. $J < J_{0.5}$ is described above. $J \geqslant J(2\mu_{0.5}, \sigma)$ implies $Y_{ox} = 0$. Figure 3's odd symmetry suggests the image variables $Y^*_{ox}/Y_{ox,\infty} \equiv 1 - Y_{ox}/Y_{ox,\infty}$ and $\mu^*/\mu_{0.5}$. Since equation (10) is only valid for $J \leqslant J_{0.5}$, an image J^* is required for any $J > J_{0.5}$. This J^* in equation (10) yields a $Y^*_{ox}/Y_{ox,\infty}$ and the desired $Y_{ox}/Y_{ox,\infty} = 1 - Y^*_{ox}/Y_{ox,\infty}$. To find J^*, first convert the known J to a μ using Fig. 2, then μ to μ^* from the above definition and finally μ^* to J^* again from Fig. 2. Since $r \leqslant 1$, $\mu_{0.5} \lesssim 0.3$ and $J(2\mu_{0.5}, \sigma) \lesssim 0.6$ from Fig. 2 which also shows that for $0.4 \lesssim J \lesssim 0.6$, $\mu = J$. For $J_{0.5} \leqslant J \lesssim 0.4$, i.e. $0 \lesssim \mu \lesssim 0.4$ in Fig. 2, a second order fit $\mu(J)$ is used

$$\mu = [(0.4\mu_{0.5} - 0.4\mu_{0.5}\sigma^2 - J^2_{0.5} + 0.1\sigma^2)(J - 0.4\sigma) + (J_{0.5} - 0.4\sigma - \mu_{0.5} + \sigma\mu_{0.5}) \times (J^2 - 0.16\sigma^2)]/[(J_{0.5} + 0.4\sigma^2)(0.4 - J_{0.5}) + \sigma(J^2_{0.5} - 0.16)]. \quad (13)$$

This μ gives a μ^* in the range 0–$\mu_{0.5}$. Writing equation (13) in terms of μ^* and J^* and inverting gives $J^*(\mu^*)$ which, with the μ^* found above, gives the required $0 \leqslant J^* \leqslant J_{0.5}$.

In summary, turbulent transport equations are used to obtain J and g at each point in the flow field. Equation (9) gives $\mu_{0.5}$ in terms of the parameter r and equations (10)–(12) yield $Y_{ox}(Y_{ox,\infty}, r, J, g)$. The remaining species and temperature time-mean variables are then given explicitly by equations (6)–(8) as functions of Y_{ox}, J, g, r and D_3. Systems which can not be approximated with a clipped Gaussian pdf [10] require more general expressions than equations (10–(12).

REFERENCES

1. D. B. Spalding, Concentration fluctuations in a round turbulent free jet, *Chem. Engng Sci.* **26**, 95–106 (1971).
2. S. E. Elghobashi and W. M. Pun, A theoretical and experimental study of turbulent diffusion flames in cylindrical furnaces, in *Fifteenth International Symposium on Combustion*, 1353–1365. The Combustion Institute (1974).
3. F. C. Lockwood and A. S. Naguib, The prediction of the fluctuations in the properties of free, round-jet turbulent, diffusion flames, *Combust. Flame* **24**, 109–124 (1975).
4. T. M. Shih and P. J. Pagni, Wake turbulent flames, ASME paper 77-HT-97 presented at the *Seventeenth National Heat Transfer Conference* (14–17 August, 1977).
5. F. Tamanini, The prediction of reaction rates and energy transfers in turbulent fire plumes, Factory Mutual Research, Technical Report, Serial No. 22360-3, RC-B-60 (May 1976).
6. W. R. Hawthorne, D. S. Weddell and H. C. Hottel, Mixing and combustion in turbulent gas jets, in *Third International Symposium on Combustion*, 266–288 (1950).
7. F. C. Lockwood and A. O. O. Odidi, Measurement of mean and fluctuating temperature and of ion concentration in round free-jet turbulent diffusion and premixed flames, in *Fifteenth International Symposium on Combustion*, 561–572. The Combustion Institute (1974).
8. F. H. Champagne, Y. H. Pao and I. J. Wygnanski, On the two-dimensional mixing region, *J. Fluid Mech.* **74**(2), 209–250 (1976).
9. P. J. Pagni and T. M. Shih, Excess pyrolyzate, in *Sixteenth International Symposium on Combustion*, 1329–1343. The Combustion Institute (1977).
10. W. B. Bush and F. E. Fendell, On diffusion flames in turbulent shear flows, *Acta Astronautica* **1**, 645–666 (1974).

Int. J. Heat Mass Transfer. Vol. 21, pp. 821–824

0017-9310/78/0601-0821 $02.00/0

TIME DEPENDENT SOLIDIFICATION OF BINARY MIXTURES*

BRUNO A. BOLEY
Technological Institute, Northwestern University, Evanston, IL, U.S.A.

(*Received* 16 *July* 1977 *and in revised form* 4 *November* 1977)

NOMENCLATURE

- A, parameter characterizing the liquidus line [equation (18)];
- B, $= (\kappa/D)^{1/2}$ [equation (13)];
- c, specific heat;
- C, mass-fraction of solute;
- D, diffusion coefficient;
- f, function;
- k, partition coefficient;
- K, thermal conductivity;
- l, latent heat of fusion;
- L, thickness;
- m, slope of liquidus line;
- M, principal fusion parameter [equation (18)];
- Q, heat flux;
- s, position of solid–liquid interface [ξ, equation (10a)];
- t, time [y, equation (10a)];
- T, temperature [V, equations (16)];
- x, distance from exposed surface [X, equation (13)].

Greek symbols

- δ, $(\kappa_S/\kappa_L)^{1/2}$ [equation (13)];
- η, ratio of liquid to solid diffusivities [equation (18)];
- κ, diffusivity;
- λ, similarity coefficient in constant surface temperature solution;
- ρ, density.

* This work was supported by the Office of Naval Research.

INTRODUCTION

THE PROBLEM of solidification (or melting) of mixtures has received attention for a number of years both from fundamental and practical points of view (cf. [1]). Analytical solutions of the corresponding coupled heat- and mass-transfer boundary-value problem have been discussed for semi-infinite bodies under sudden changes of surface temperature (e.g. [2–4]). The response to these special conditions has been found to be characterized by similarity, and by constancy of concentration in the solid, and in both phases at the interface. The present work examines a slab, solidifying under arbitrarily time-dependent cooling conditions at the surface, and derives a solution in series form. Neither similarity nor the special behavior alluded to earlier prevails in this solution.

FORMULATION OF THE PROBLEM

Consider a slab ($0 < x < L$), initially ($t = 0$) liquid with temperature T_{L0} and with solute concentration C_{L0}, under prescribed cooling conditions at $x = 0$ and (to fix ideas)